Fall 12-2017

The Impact of Delay on Retrieval Success in the Parietal Memory Network

Nathan Anderson
Washington University in St. Louis

WASHINGTON UNIVERSITY IN ST. LOUIS
Department of Psychological & Brain Sciences

The Impact of Delay on Retrieval Success in the Parietal Memory Network

by
Nathan L. Anderson

A thesis presented to
The Graduate School
of Washington University in
partial fulfillment of the
requirements for the degree
of Master of Arts

December 2017
St. Louis, Missouri

Table of Contents

List of Figures

List of Tables

Acknowledgments

I'd like to achnowledge and thank my advisor, Kathleen McDermott, for all of her guidance and help in completing this project. I'd also like to thank the members of my lab, including Adrian Gilmore, Hank Chen, Christopher Zerr, Thomas Spaventa, Ruthie Shaffer, and Jeff Berg for their invaluable assistance.

I'd like to thank Dart Neuroscience for their generous funding, which made this project possible.

I offer special thanks to the Washington University School of Engineering for allowing me to use their dissertation and thesis template as a starting point for the development of this document.

Nathan L. Anderson

Washington University in St. Louis

December 2017

Dedicated to my wife, Stephanie.

ABSTRACT OF THESIS

The Impact of Delay on Retrieval Success in the Parietal Memory Network

by

Nathan L. Anderson

Master of Arts in Psychological & Brain Sciences

Washington University in St. Louis, 2017

Professor Kathleen B. McDermott, Chair

Recent work has identified a Parietal Memory Network (PMN), which exhibits regular patterns of activation during memory encoding and retrieval. Among these characteristic patterns, this network displays a strong "retrieval success" effect, showing greater activation for correctly-remembered studied items (hits) compared to correctly-rejected novel items (CRs). To date, most relevant studies have used short retention intervals. Here, we ask if the retrieval success effect seen in the PMN would remain consistent over a delay. Twenty participants underwent fMRI while encoding and recognizing scenes. Greater activity for hits than for correctly-rejected lures within PMN regions was observed after a short delay (~10 min), replicating prior reports. However, after a long retention interval (~48 hours), the network showed an attenuated (but still present) retrieval success effect, with the disparity driven primarily by attenuated activation for hits (i.e., correctly-rejected lures exhibited little to no activity at both delays). Importantly, this difference cannot be entirely explained by a decrease in participant confidence after the delay. These findings suggest a degree of temporal constraint on experiences with stimuli that elicit activation in the PMN.

Chapter 1: Introduction

In fMRI studies of memory, the retrieval success effect has often been used to identify areas of the brain important for memory retrieval. “Retrieval success” refers to a positive contrast between activation when a subject successfully remembers a studied (or old) item during a test, and when a subject correctly rejects an nonstudied (or new) item. That is, the contrast assesses the difference between activity elicited by the experience of successful retrieval relative to a failed attempt to remember. This contrast has identified regions within medial and lateral parietal cortex that show retrieval success effects in recognition tasks (e.g. Henson, Rugg, Shallice, & Dolan, 2000; Konishi, Wheeler, Donaldson, & Buckner, 2000; McDermott, Jones, Petersen, Lageman, & Roediger, 2000; Wheeler & Buckner, 2004). Conspicuously absent in studies of retrieval success are regions in the hippocampus and medial temporal lobe (MTL; Henson, 2005).

Recent meta-analyses have solidified the conclusions that midline and lateral parietal cortex are robustly active during retrieval. In work by Kim (2013), 48 task-based studies from the literature were subjected to a quantitative meta-analysis. Among the regions produced by Kim’s analysis were those within bilateral posterior cingulate cortex, bilateral precuneus, and left angular gyrus. McDermott and colleagues showed in a meta-analysis that laboratory-based memory experiments (as opposed to autobiographical memory experiments) found a retrieval success effect in regions within the left precuneus and bilateral inferior parietal lobule, as well as posterior cingulate cortex (McDermott et al., 2009). In another meta-analysis on a separate set of data, Nelson et al. (2010) studied retrieval success in left lateral parietal cortex, and identified

regions within the left posterior inferior parietal lobule that task-based paradigms often found in conjunction with regions in left precuneus and posterior cingulate cortex.

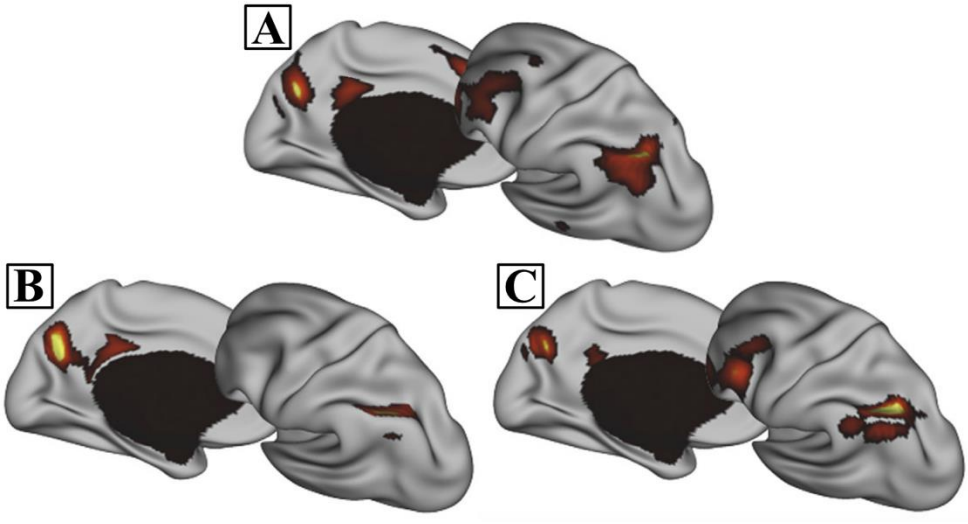

Figure 1.1: Meta-analyses of retrieval success, demonstrating activation in medial and lateral parietal cortex. **A)** Kim et al. (2013) **B)** Nelson et al. (2010) **C)** McDermott et al. (2009). *Figure adapted from Figure 1 of Gilmore et al. (2015)*

These studies and meta-analyses have convincingly identified sets of commonly co-occurring regions that emerge from memory-related contrasts using task-based fMRI (i.e., fMRI studies in which participants are given a specific task and regions of activation are determined from various task conditions and response types). A related but parallel line of neuroimaging work, resting state functional connectivity MRI (rsfc-MRI), has made great strides in identifying coherent brain networks independent of specific task demands. This approach focuses on the slow fluctuations in brain activity (<0.1Hz) that occur when an individual is at rest (i.e. aware, but not asked to do any cognitive task), and determines which regions of the brain tend to activate and deactivate in sync (i.e. in a temporally correlated manner; Greicius et al., 2003; Power et al., 2011; Yeo et al., 2011); for a review, see Power et al., 2014). This co-activation has been used to argue for functional (if not strictly physical) connections between regions, which

can be used to organize the brain into a map of separable networks using graph theoretic approaches (see Power, Schlaggar, & Petersen, 2014).

The results from rsfc-MRI have been used in conjunction with task-based MRI to make claims of functionally-related, separable brain networks. For example, significant work on the "default mode" of the brain initially used task-based fMRI to identify a collection of regions (including those within medial frontal cortex, posterior cingulate cortex, precuneus, angular gyrus, and MTL) that show consistent patterns of deactivation in response to goal-directed behaviors (Raichle et al., 2001; Shulman et al., 1997). Later rsfc-MRI work independently identified a similar set of regions without the use of any "relevant" tasks, helping to define the "default mode network" (DMN) as a functional brain network (Fox et al., 2005; Greicius, Krasnow, Reiss, & Menon, 2003). This is important, as it implies emergence of this network over a lifetime of co-activation. The use of functional connectivity and task-based MRI, taken together, provide strong evidence for the existence of a discrete default mode network that supports specific mental processes. Similar convergence has been found for multiple other brain networks (e.g. the dorsal attention network; frontal-parietal control network; cingulo-opercular network; ventral attention network)

As resting-state functional mapping of the brain progressed, networks were identified that were not yet clearly classified based on the task-MRI literature. Among these was a collection of regions in lateral and medial parietal cortex, identified by multiple rsfc-MRI studies (Doucet et al., 2011; J. Power et al., 2011; Shirer, Ryali, Rykhlevskaia, Menon, & Greicius, 2012; Smith et al., 2013; Yeo et al., 2011). Notably, Power et al. (2011) and Power et al. (2014) identified this

network of parietal regions "with previously unknown functional identit[y]," and speculated that it was involved in memory retrieval based on meta-analysis.

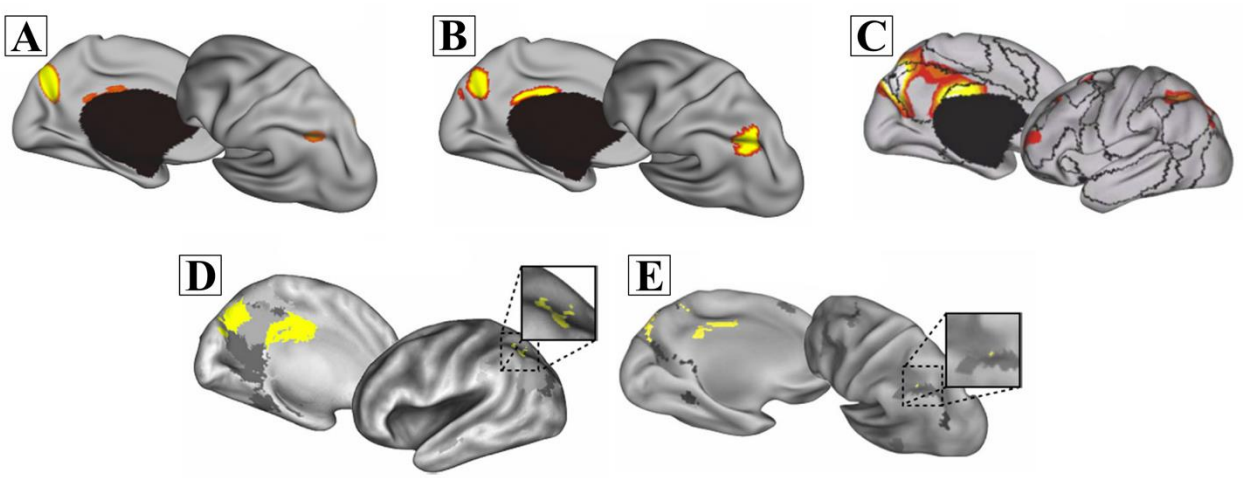

Figure 1.2: Network of parietal regions revealed through resting-state functional connectivity analyses. **A)** Human Connectome Project (Smith et al., 2013) **B)** Shirer et al. (2012) **C)** Yeo (2001) **D)** Doucet et al. (2011) **E)** Power et al. (2011)
Figure adapted from Gilmore et al. (2015)

A review by Gilmore, Nelson, and McDermott (2015) sought to integrate the results from the task-based and connectivity MRI literatures regarding parietal cortex and its role in memory. Looking back at the work of the previous meta-analyses of retrieval success effects (Kim, 2013; McDermott et al., 2009; Nelson et al., 2010), it became clear that a similar set of parietal regions identified in functional connectivity studies was also found when using a retrieval success contrast (remembered old items > correctly-rejected new items). The results provided by previous task-based MRI and rsfc-MRI studies were synthesized; the regions of overlap occurred within the precuneus (PCU), mid-cingulate cortex (MCC), and posterior inferior parietal lobule (pIPL, sometimes labeled as dorsal angular gyrus). Given their establishment as a functional network, and their support of memory processes (beyond just the retrieval success effect), this set of regions was called the "Parietal Memory Network." Importantly, the authors noted that this

network was distinct from the DMN, but that all regions of the PMN are immediately adjacent to those of the DMN (Gilmore et al., 2015, Figure I). This spatial proximity helps provide some explanation for its occasional inclusion in earlier studies of the DMN, which also demonstrates memory effects (see Figure 1.3).

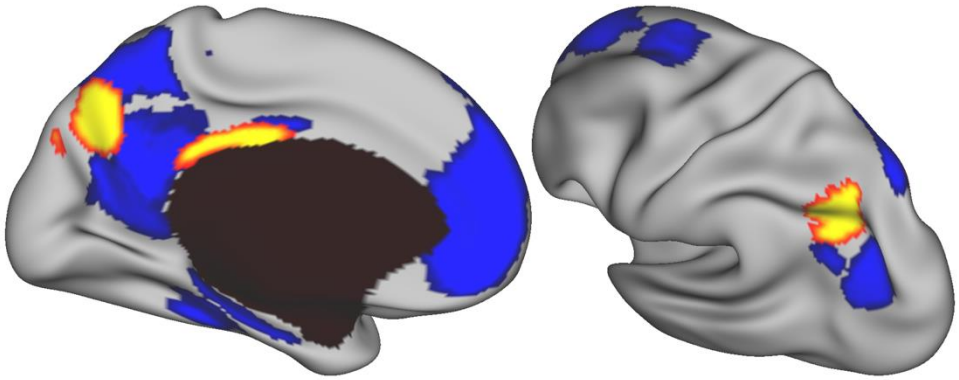

Figure 1.3: The extent of the Parietal Memory Network (yellow) and Default Mode Network (blue). Note the spatial proximity of the two networks.
Regions from Shirer et al. (2012) available at https://findlab.stanford.edu/functional_ROIs.html

In addition to the retrieval success effect, other patterns of activity help to define this newly-acknowledged network as being memory-related. For example, it shows deactivation during encoding when an individual is exposed to novel stimuli (that is, stimuli that is novel within the context of the experiment), with greater deactivation for stimuli that will later be remembered compared with that which will later be forgotten (i.e. missed on a recognition test; Kim, 2011; Nelson, Arnold, Gilmore, & McDermott, 2013; Otten & Rugg, 2001). This deactivation during encoding, along with the typical activation for hits during retrieval, has led to the PMN being described as demonstrating an "encoding/retrieval flip."

Previous work has determined that PMN regions show greater activation for items that exhibit relatively greater memory strength; for example, when material is restudied again before

testing (Nelson, Arnold, Gilmore, & McDermott, 2013). However, it is important to note that this is not a measure of absolute memory strength; when word lists are studied during the experiment, the words are not entirely novel to the participant. As noted above, PMN regions will still show deactivation during encoding even when the stimulus is already known the individual (for example, when being instructed to remember a word in a list that is already in the indiviual's vocabulary). Therefore, the "memory" being tested is rather that of a specific past experience with the stimulus, and the activity in the PMN must—to some degree—reflect a temporally- or episodically-constrained assessment of the item's memory strength. However, the majority of previous experiments studying activity in PMN regions have done so with relatively short timeframes, using a single experimental context/session and retention intervals that span no more than a few hours.

Another important consideration for memory research (especially over longer delays) is the question of confidence. Over longer retention intervals, it is expected that confidence will decrease even for correctly-remembered items (e.g. Haist, Shimamura, & Squire, 1992). Additionally, studies of memory which include contrasts of confidence levels have revealed parietal regions now known to fall within the PMN (Hutchinson, Uncapher, & Wagner, 2015; Yonelinas, Otten, Shaw, & Rugg, 2005). Therefore, collection of confidence ratings and accounting for their influence will be an important factor in determining the impact (if any) of longer retention intervals on PMN activity.

The purpose of this experiment is to investigate the PMN's role in memory for items that are tested after a longer delay by having subjects return to be tested after 48 hours. If activity in the PMN reflects some form of temporally-constrained memory strength that is specific to the experimental context, we can expect the retrieval success effect to be attenuated (or lost) after a

longer delay, due to the increased time between the retrieval task and the initial episodic experience. However, if the memory signal represented in the PMN is effectively acontextual with respect to the initial study experience, the pattern of activation could be similar to that seen at a relatively short delay.

Chapter 2: Method

2.1 Participants

Thirty participants (16 female, ages 18-31) were recruited from Washington University and the St. Louis area. Participants were all right-handed, native speakers of English (learned by age 5), had normal or corrected-to-normal vision, and had no history of psychiatric or neurological disorders. Participants' data was excluded for the following reasons: 3 for a software error, 1 for a hardware error, 1 for excessive sleepiness during the tasks, 1 for large (but benign) ventricle abnormalities, and 4 for excessive motion. This leaves a final sample of $N = 20$. Informed consent was obtained for all participants, and the study was conducted in accordance with Washington University human research practices. Participants were paid $25 per hour.

2.2 Materials

Five hundred and seventy-six images were selected as stimuli. These were gathered via Google Images (images.google.com) using the procedure described in Konkle, Brady, Alvarez, & Oliva (2010) (a subset of the images used in this experiment were gathered for the experiment described in Chen, Gilmore, Nelson, & McDermott, 2017). Images were 800 x 600 pixels, with an overall screen resolution of 1024 x 768. 288 of the images depicted outdoor scenes, while the remaining 288 depicted indoor scenes; none of the scenes contained people. Scenes were counterbalanced to appear in different sessions, task types (encoding or retrieval), and states (studied or nonstudied) across participants.

2.3 Encoding and Retrieval Instructions and Procedures

The procedure used in this experiment is shown in Figure 2.1 (task design) and Figure 2.2 (overall experiment design). The experiment consisted of two sessions, separated by

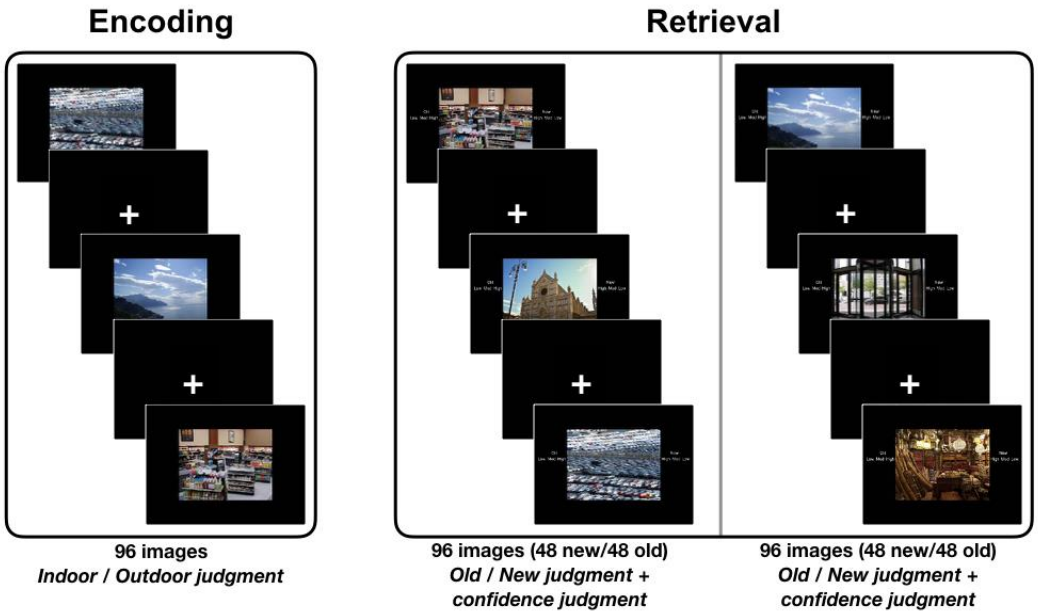

Figure 2.1: Task design for encoding and retrieval blocks

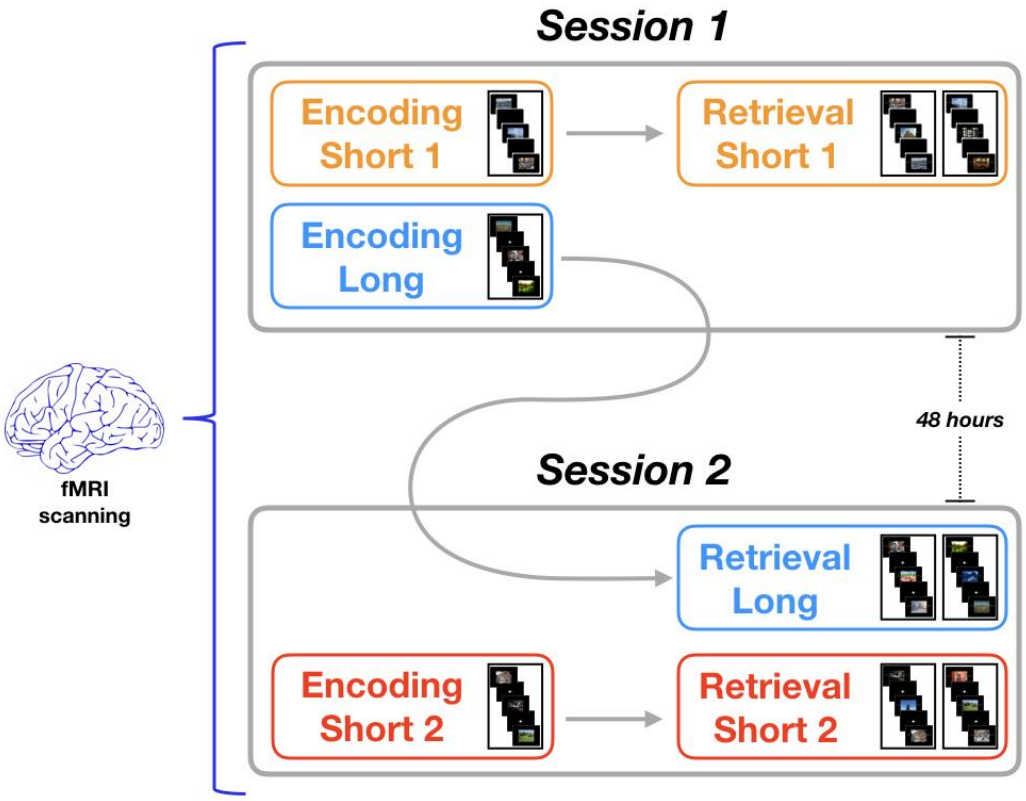

Figure 2.2: Experiment design

approximately 48 hours (range = 46-50 hours). All tasks during both sessions were conducted entirely within the scanner.

During Session 1, participants began with an encoding task (Encoding Short 1) in which they were shown 96 scenes (48 indoor, 48 outdoor). Scenes were displayed for 0.5s, with 0-6 (jittered) fixation frames presented between each stimulus. For each scene, participants were asked to determine if the image depicted an indoor scene or an outdoor scene, and make a response on a button box.

Following this task, participants performed a retrieval task (Retrieval Short 1) in which they were shown 96 old studied scenes (from Encoding Short 1) and 96 new nonstudied scenes across two scanner runs. Scenes were presented for 1.9s, with 0-6 (jittered) fixation frames presented between each stimulus. In addition, reminder text was displayed to the immediate right and left of each presented image, which reminded the participant of the response mappings for their button box. For each image, participants were asked to determine if the image was old (previously seen during Encoding Short 1) or new. In addition, they were asked to make a confidence judgment in their decision, with response options of High, Moderate (Mod), and Low confidence. As a result, participants could make one of six responses (Old-High, Old-Mod, Old-Low, New-High, New-Mod, or New-Low).

For the final task in Session 1, participants perfomed another encoding task (Encoding Long) identical to the previously-described Encoding Short 1 task. This task contained 96 new scenes.

During Session 2 (48 hours later), participants performed another retrieval task (Retrieval Long). This included the images from the Encoding Long task (performed during the previous session), as well as 96 nonstudied foil images.

After this task was complete, participants completed a final round of encoding (Encoding Short 2) and retrieval (Retrieval Short 2) tasks, exactly as described above, with a new set of studied images.

Additionally, 7 minutes of resting state data was collected at the beginning and end of Session 1 (total: 14 minutes), and another brief experiment was conducted at the conclusion of Session 2. These data are not reported here.

2.4 fMRI Data Acquisition

Functional and structural scans were acquired on a Siemens 3.0T Prisma system using a Siemens 32-channel head coil. Stimuli were presented using PsychoPy (Peirce, 2007) on an iMac or Macbook Air computer, which received sync pulses from the scanner. Sync pulses were used by PsychoPy to determine onset of stimuli presentation to the participant's screen. Length of jitter and randomization of trial types were optimized using the program OptSeq2 (http://surfer.nmr.mgh.harvard.edu/optseq).

Structural images were acquired during the first session, using a T1-weighted sagittal MPRAGE (TE, 2.22ms; TR, 2400ms; TI, 1000ms; flip angle, 8°; 208 slices with resolution 0.8 x 0.8 x 0.8 mm voxels).

Functional imaging used a BOLD contrast sensitive gradient-echo echoplanar sequence (TE, 27ms; flip angle, 50°; in-plane resolution, 3 x 3 mm). Whole-brain EPI volumes (MR

frames) of 48 contiguous, 3-mm-thick axial slices were obtained every 1.1s, using a multi-band factor of 4. Slice acquisition order was interleaved, with a slice gap of 0. Each functional run (encoding or retrieval) consisted of 314 frames. The first eight functional images of each scan were discarded to allow for T1 equillibration effects.

2.5 Analysis and Visualization Software

Imaging analysis (including all preprocessing, GLM coding, and statistical analyses) was done using the software package Analysis of Functional NeuroImages (AFNI; http://afni.nimh.gov/afni/; Cox, 1996; version 17.1.12). All reported atlas coordinates are in MNI 152 space. Figures displaying statistical maps were made by projecting and displaying the volumetric data onto a partially inflated representation of the human brain using the Connectome Workbench software (Marcus et al., 2011). Additionally, verbal labels of resulting activations are provided by AFNI's *whereami* program.

2.6 fMRI Data Preprocessing

The following list contains preprocessing steps, including the AFNI program used: uniformity correction on the anatomical image to prepare for later nonlinear warping (*3dUnifize*), despiking of functional images (*3dDespike*), skull-stripping of anatomical images (*3dSkullStrip*), alignment of functional images to their respective anatomical images (*@Align_Centers* and *align_epi_anat.py*), transformation of functional and anatomical images into MNI space using non-linear warping, along with volume registration to the third frame of the first functional scan (*auto_warp.py*, *3dvolreg*, and *3dNwarpApply*), blurring of functional images using a Gaussian smoothing kernel with 4.0mm FWHM (*3dmerge -1blur_fwhm*), and scaling to a mean of 100 to allow for group comparisons (*3dcalc*).

2.7 GLM coding

For the analyses reported here, only the retrieval data will be included.

The data were modeled with a general linear model, which included 4 regressors of interest: old studied items correctly judged to be old (remembered items, or "Hits"), new nonstudied items correctly judged to be new (correctly rejected items, or "CRs"), old items incorrectly judged to be new (forgotten items, or "Misses") and new items incorrectly judged to be old (false alarms, or "FAs"). For each participant, RTs for each trial were included as a regressor of no interest. Six additional regressors of no interest were included to control for motion (x/y/z translation and yaw/pitch/roll). A gamma function was used to estimate the hemodynamic response for each condition (AFNI default for gamma function: height of 1, duration of approximately 12 seconds). Effects were analyzed in terms of percent signal change relative to baseline.

Similar GLMs were created in which Hits and CRs were divided by confidence level. Six regressors of interest were used: Hits (High confidence), Hits (Moderate or Low confidence), CRs (High Confidence), CRs (Moderate or Low confidence), Misses, and FAs. In these GLMs, misses and FAs were not separated by confidence due to a lack of responses and their use only for completeness in labeling all event types, rather than use for later statistical analyses. Due to a lack of responses in one or more bins for hits or CRs, 4 additional subjects were excluded from this analysis (final $N = 16$). As a result, all participants had a minimum of 4 trials in each bin. All other analysis was performed identically to the basic GLM modeling described above.

2.8 Voxelwise *t*-test analysis and ANOVA approach

Unless otherwise specified, all *t*-test images were thresholded to $p < .001$, using a cluster size threshold yielding $\alpha < .05$. The minimum number of contiguous voxels for surviving clusters was determined using AFNI's *–Clustsim* option in the program *3dttest++*, which simulates 1000 null results to control for the false positive rate. This new procedure avoids the issues described in Eklund, Nichols, & Knutsson (2016), addressing incorrect assumptions regarding the shape of the spatial auto-correlation function.

Our analysis began with 3 whole-brain *t*-tests, in which the retrieval success effect (Hit-CR) was examined for each of the test conditions (2 short delays, 1 long delay). This step primarily establishes that the results from the short retrieval interval conditions conform to expectations from the literature, giving confidence to the follow-up analyses.

In order to isolate PMN regions and determine the effect of delay on the activity within these regions, two masks were created from the Retrieval Short 1 data from the first session. The rationale for these masks was to restrict the search space for the analysis of variance to voxels that conformed to known patterns within the Parietal Memory Network and avoiding the adjacent Default Mode Network. Specifically, we examined only voxels that exhibited *both* a retrieval success effect (Hit > CR) and above-baseline activity for hits. Many regions in the default mode network (DMN) are adjacent to the PMN (as seen in Figure 1.3), but the DMN shows a characteristic decrease below baseline in activity for externally-oriented tasks, such as recognition memory tests (Shulman et al., 1997). Thus, this mask should exclude canonical DMN regions. Using the Session 1 short-retention interval data (Retrieval Short 1) for region definition permits the independent assessment of the Session 2 data (Retrieval Short 2 and

Retrieval Long); in other words, the data used for mask creation is separate from the ANOVA analysis data[1].

Specifically, the first mask consisted of voxels demonstrating significantly greater activity for hits than for CRs ($p < .05$, uncorrected for multiple comparisons). The second mask contained voxels that showed above-baseline activity for hits ($p < .05$, uncorrected). A conjunction of these two masks was created, which included only voxels showing both Hit > CR and Hit > Baseline effects.

A 2x2 factorial ANOVA was then performed on the Retrieval Long (long delay) and Retrieval Short 2 (short delay) data from the second session using AFNI's *3dANOVA3* program. The ANOVA was only performed on voxels that fell within the conjunction mask produced from the independent first-session data. The factors of interest were response type (Hit x CR) and delay (Short x Long). ANOVA results were thresholded at $p < .01$, and we only consider clusters with at least 5 contiguous voxels.

Though we consider main effects of delay and retrieval success, of most interest were clusters that showed an interaction; these were used as ROIs to calculate average magnitudes. Within each cluster, the percent signal change was determined for each participant for each response of interest (Short-delay hits, short-delay CRs, long-delay hits, and long-delay CRs) and averaged across participants to better determine the source of the significant interaction. T-tests

[1] In order to ensure that Retrieval Short 1 and Retrieval Short 2 tests were similar, and that our results were not biased by selecting the first session's data for creating our masks, whole-brain t-tests were perfomed comparing activation for hits between Retrieval Short 1 and Retrieval Short 2, as well as comparing retrieval success measures (Hit-CR) between Retrieval Short 1 and Retrieval Short 2. Both t-tests showed no significant clusters after correction.

were perfomed on these magnitude estimates in order to determine significant differences amongst individual conditions.

Chapter 3: Results

3.1 Behavioral results

Participants were fairly accurate during both of the short-delay recognition tests, with average hit rates of .71 (Retrieval Short 1) and .70 (Retrieval Short 2). Hit rates decreased on the long-delay test (M = .56) (See Figure 3.1). Correct rejection rates showed a similar pattern (Retrieval Short 1 M = .86; Retrieval Short 2 M = .82; Retrieval Long M = .74). When separated by confidence (eliminating the four disqualified participants, noted above), responses show that there was a significantly smaller proportion of high-confidence hits on the long-delay test, when compared to either short-delay test (test for equality of proportions; Retrieval Short 1 vs Retrieval Long: $X^2 = 13.21$, $p < .001$; Retrieval Short 2 vs Retrieval Long: $X^2 = 6.17$, $p < .05$) (see Figure 3.2). A similar pattern was seen for high-confidence CR responses only between Retrieval Short 1 and Retrieval Long (Retrieval Short 1 vs Retrieval Long: $X^2 = 4.37$, $p < .05$; Retrieval Short 2 vs Retrieval Long: $X^2 = 0.72$, $p = .40$)[1].

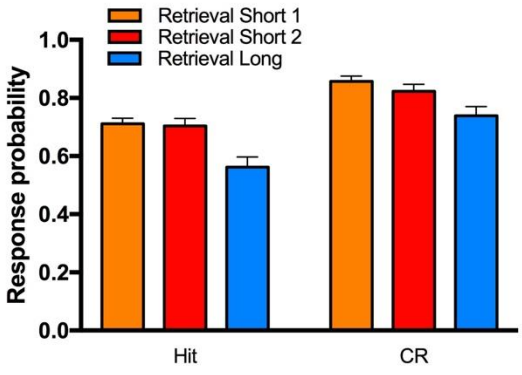

Figure 3.1:
Behavioral results, collapsing across confidence
(N = 20)

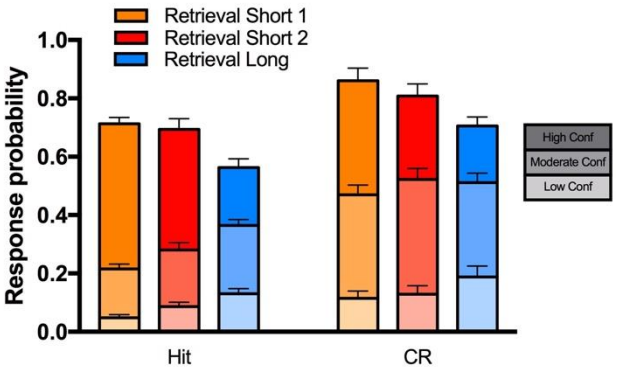

Figure 3.2:
Behavioral results, separated by confidence
(N = 16)

[1] Figures including miss and FA response types can be seen in the Appendix (Figure A.1 and A.2).

3.2 Whole-brain *t*-tests

The presence of a retrieval success effect was established in a series of three whole-brain *t*-tests: Retrieval Short 1 Hit-CR, Retrieval Short 2 Hit-CR, and Retrieval Long Hit-CR. The statistical maps for these three tests can be seen in panels A-C of Figure 3.3. Notably, we see the regions comprising the PMN (bilateral precuneus, mid-cingulate, and pIPL) emerge in all three conditions, along with others such as the left medial frontal gyrus. Panel D shows the results of a task-based meta-analysis from Kim (2013), showing activation corresponding to the retrieval success effect – the regions shown in this panel are consistent with those found in our study, as would be expected for the short retention interval condition. The data in Panel C suggest similar effects are seen after a long retrieval interval. Based on these results, it is clear that the PMN is relevant to the study of the retrieval success effect in this context, and we proceeded to a more targeted analysis to investigate its role.

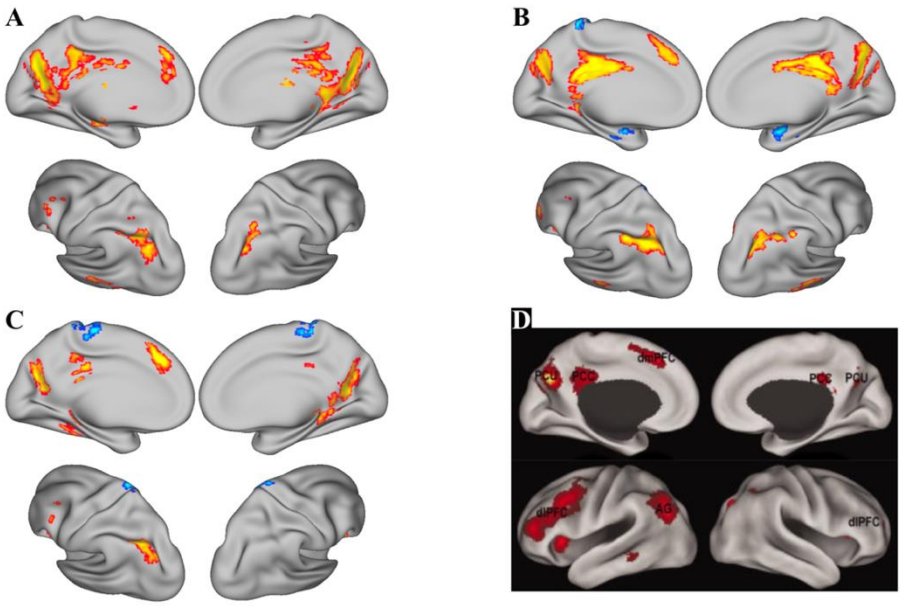

Figure 3.3: Whole-brain t-tests of Hit-CR. Warm colors show Hit > CR, while cool colors show CR > Hit. **A)** Retrieval Short 1; **B)** Retrieval Short 2; **C)** Retrieval Long. **D)** Adapted from Figure 1 of Kim, 2013 showing a retrieval success effect across 48 studies.

3.3 Mask Creation

As described in section 2.8, a mask was created in order to target our investigation to PMN regions. Two initial masks were created from the Retrieval Short 1 data, with the goal of then examining the independent Retrieval Short 2 and Retrieval Long data. The first mask was generated from a *t*-test of Hit > CR ($p < .05$, uncorrected for multiple comparisons) (Figure 3.4, in blue), and the second was generated from a *t*-test of Hit > Baseline activity ($p < .05$, uncorrected) (Figure 3.4, in yellow). The conjunction of these two masks was then determined, with the final mask containing only voxels that were present in both initial masks (i.e., only voxels showing both greater activation for hits than CRs, and activation above baseline for hits; see green in Figure 3.4). This mask was then used to perform the 2x2 ANOVA analysis on the Retrieval Short 2 and Retrieval Long data, allowing for PMN localization based on an independent dataset within the same subject sample.

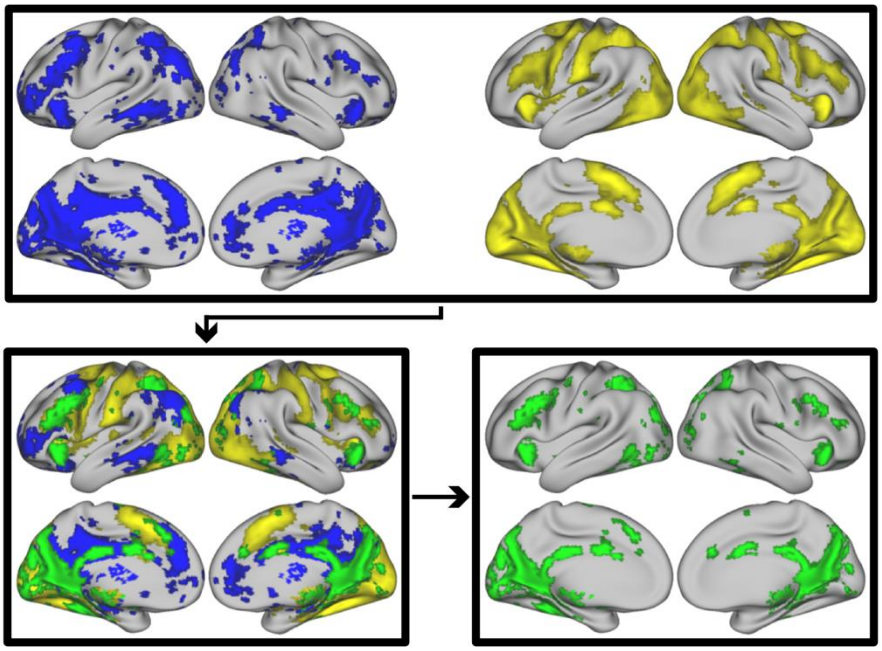

Figure 3.4: Masks created for ANOVA approach. All data are from Retrieval Short 1. Blue: Hit > CR ($p < .05$); Yellow: Hit > Baseline ($p < .05$); Green: overlap of blue and yellow. Subsequent analyses were masked by the voxels shown in green.

3.4 ANOVA Analysis

3.4.1 Statistical Maps

A 2x2 ANOVA was performed within the masked regions for the Retrieval Short 2 and Retrieval Long data (Hit/CR vs Short delay/Long delay). The statistical maps illustrating the main effects of the ANOVA analysis are shown in Figure 3.5, while the interaction is shown in Figure 3.6. Regions that showed a main effect of Hit vs CR are listed in Table 3.1, while regions showing a main effect of Short vs Long delay are listed in Table 3.2. There is a strong main effect of Hit vs CR, with PMN regions appearing bilaterally (Figure 3.5, Panel A). The map for the main effect of delay is less robust, but bilateral precuneus and left pIPL are still visible (Figure 3.5, Panel B). Most notably, the interaction (Figure 3.6) reveals PMN regions, including bilateral precuneus and mid-cingulate as well as left pIPL. Additionally, an interaction was seen in bilateral parahippocampal gyrus and right superior parietal lobule (see Table 3.3).

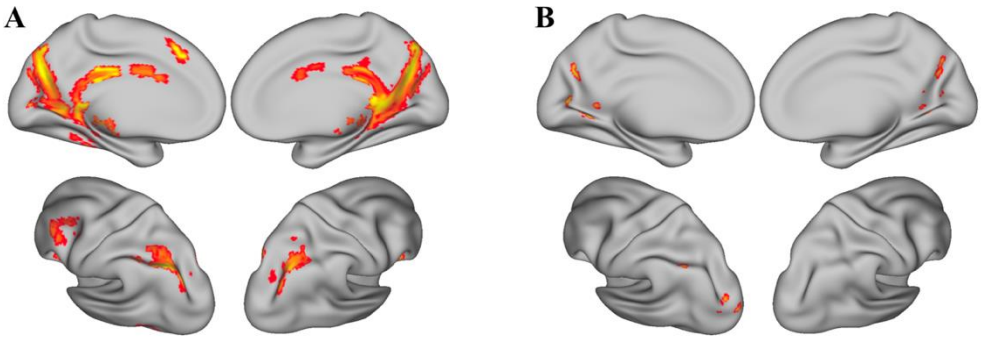

Figure 3.5: Statistical maps from the masked ANOVA analysis of the **A)** Main effect of Hit vs CR; **B)** Main effect of Short delay vs Long delay

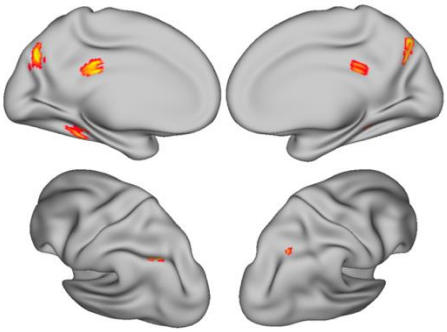

Figure 3.6: Statistical map of the interaction from the masked ANOVA analysis – (Hit vs CR) x (Short delay vs Long delay)

Table 3.1: Center-of-mass coordinates for regions exhibiting a Main Effect of Hit vs CR ($p < .01$)

Region	Voxels	CM x	CM y	CM z
Bilateral Precuneus	990	2	-58	21
Left Inferior Parietal Lobule	200	-35	-62	47
Left Middle Frontal Gyrus	146	-48	17	33
Right Superior Parietal Lobule	143	35	-64	46
Right Caudate	122	11	3	6
Left Caudate	102	-12	4	8
Left Inferior Frontal Gyrus	94	-32	23	-3
Right Inferior Frontal Gyrus	84	34	25	-3
Right Declive [*Cerebellum*]	59	9	-77	-28
Left Medial Frontal Gyrus	33	-7	26	44
Left Cingulate Gyrus	29	-5	2	28
Left Middle Occipital Gyrus	28	-48	-65	-12
Left Declive [*Cerebellum*]	23	-10	-77	-30
Right Inferior Semi-Lunar Lobule [*Cerebellum*]	19	34	-71	-52
Left Parahippocampal Gyrus	17	-26	-33	-5
Left Nodule [*Cerebellum*]	13	-2	-57	-36
Right Cingulate Gyrus	13	6	6	29
Left Cuneus	12	-11	-83	7
Right Thalamus	11	7	-25	-7
Left Thalamus	9	-10	-22	13
Left Inferior Semi-Lunar Lobule [*Cerebellum*]	8	-34	-72	-53
Left Fusiform Gyrus	7	-28	-38	-22
Left Parahippocampal Gyrus	7	-28	-45	-12
Left Caudate	7	-33	-14	-8
Right Declive [*Cerebellum*]	6	33	-69	-28

Table 3.2: Center-of-mass coordinates for regions exhibiting a Main Effect of Short delay vs Long delay ($p < .01$)

Region	Voxels	CM x	CM y	CM z
Right Posterior Cingulate	15	13	-59	7
Right Precuneus	15	16	-62	32
Left Cuneus	14	-14	-71	7
Left Inferior Parietal Lobule	10	-40	-58	51
Left Middle Occipital Gyrus	8	-17	-96	12
Left Precuneus	8	-13	-64	31
Left Posterior Cingulate	7	-10	-57	3
Left Middle Occipital Gyrus	7	-28	-83	15

Table 3.3: Center-of-mass coordinates for regions exhibiting an interaction ($p < .01$)

Region	Voxels	CM x	CM y	CM z
Left Precuneus	29	-11	-72	36
Right Precuneus	28	11	-71	41
Left Parahippocampal Gyrus	20	-28	-40	-15
Right Superior Parietal Lobule	19	37	-55	50
Left Mid-cingulate	10	-6	-32	27
Left Inferior Parietal Lobule	8	-38	-61	46
Right Mid-cingulate	6	8	-34	27
Right Parahippocampal Gyrus	5	24	-38	-8.9

3.4.2 Magnitudes

For each region that showed a significant interaction, average magnitudes were calculated for each response type included in the ANOVA (short-delay hit, short-delay CR, long-delay hit, and long-delay CR). These magnitudes for PMN regions are shown in Figure 3.7. To better understand the interaction, we computed simple effects tests.

During the short delay, the retrieval success effect occurred in all regions (Short 2 Hit vs Short 2 CR; Left Precuneus: $t_{19} = 6.99$, $p < .001$; Left Mid-cingulate: $t_{19} = 6.92$, $p < .001$; Left pIPL: $t_{19} = 6.38$, $p < .001$; Right Precuneus: $t_{19} = 6.17$, $p < .001$; Right Mid-cingulate: $t_{19} = 6.50$, $p < .001$). After the long delay, the effect either disappeared (Right Mid-cingulate: $t_{19} = 0.96$, $p = .35$) or was attenuated (Left Precuneus: $t_{19} = 4.82$ $p < .001$; Left Mid-cingulate: $t_{19} = 3.28$, $p < .01$; Left pIPL: $t_{19} = 6.46$, $p < .001$; Right Precuneus: $t_{19} = 3.66$, $p < .01$). This attenuation can be determined by examining the difference between hits across the short and long delays, as well as the difference for CRs. In all cases, the degree of activation for hits was significantly greater for the short-delay than for the long-delay (Left Precuneus: $t_{19} = 3.96$, $p < .001$; Left Mid-cingulate: $t_{19} = 3.54$, $p < .01$; Left pIPL: $t_{19} = 3.61$, $p < .01$; Right Precuneus: $t_{19} = 4.09$, $p < .001$; Right Mid-cingulate: $t_{19} = 3.61$, $p < .01$). However, in all regions there was no difference in activation for CRs across the two delays (among 5 regions, greatest $t_{19} = 0.90$, $p = .38$)[2].

[2] Figures showing magnitudes for the 3 non-PMN ROIs (within SPL and bilateral parahippocampal gyrus) can be found in the Appendix (Figure A.3).

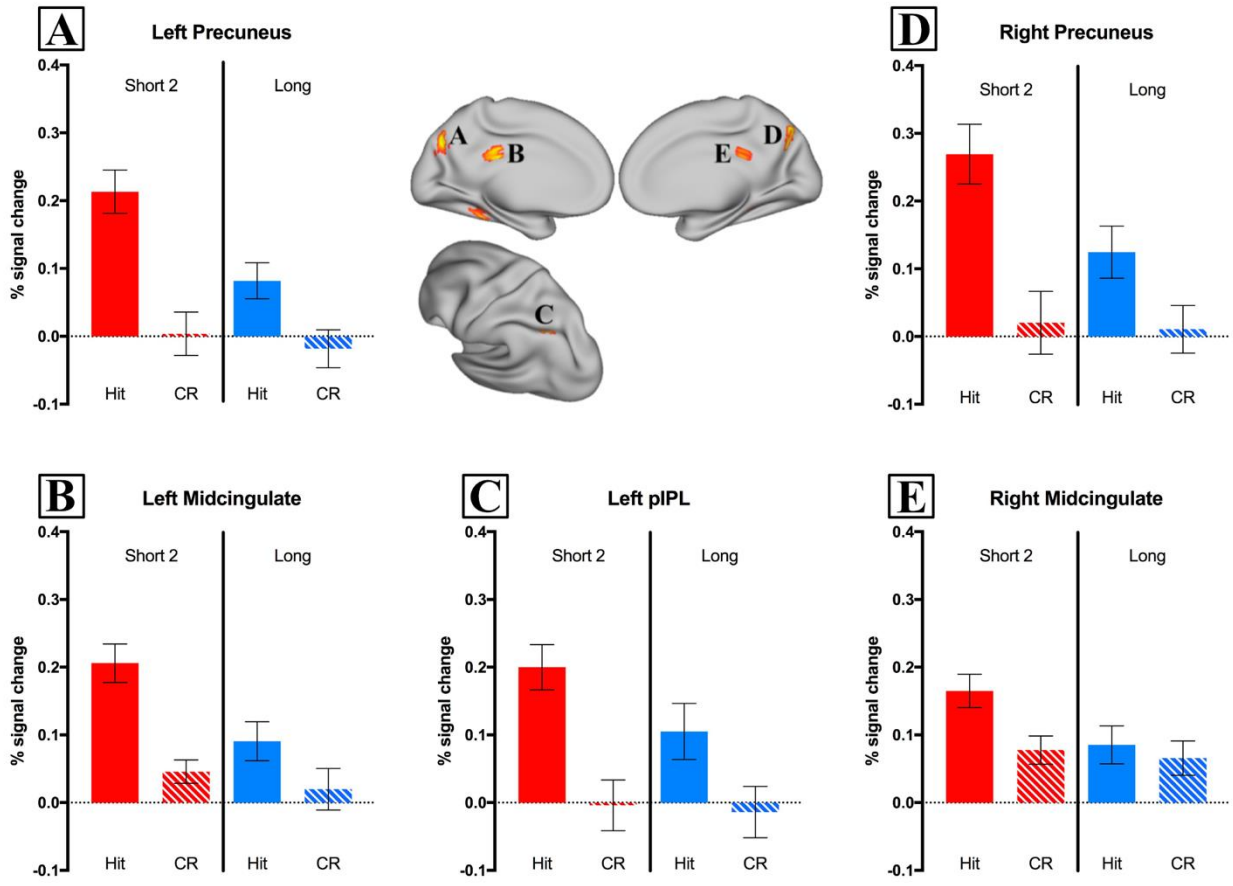

Figure 3.7: Average magnitudes for PMN regions revealed through the ANOVA interaction term.

3.4.3 Confidence

One possible confounding factor in our experiment is shown in the breakdown of the behavioral results by confidence judgment (Figure 3.2). During the long-delay condition, participants were significantly less confident in their responses (especially hits). As previous work has shown that parietal regions pertaining to the PMN are sensitive to confidence, considering confidence ratings is especially relevant to this experiment (Hutchinson, Uncapher, & Wagner, 2015; Yonelinas, Otten, Shaw, & Rugg, 2005). In order to address this issue, the same regions from the ANOVA analysis were used again as ROIs, and average magnitudes were

calculated for 16 participants with both hits and CRs separated into two confidence bins (high confidence and moderate/low confidence). These magnitudes are shown in Figure 3.8.

The results for this approach are mixed. When performing an ANOVA for Hit/CR vs Short delay/Long delay on the magnitudes within only the high-confidence bin, there is no significant interaction in any PMN region (largest $F_{(1,45)} = 0.45$, $p = .51$). There is a significant main effect of Hit vs CR in all PMN regions (Left Precuneus: $F_{(1,45)} = 27.07$, $p < .001$; Left Mid-cingulate: : $F_{(1,45)} = 14.29$, $p < .001$; Left pIPL: $F_{(1,45)} = 39.44$, $p < .001$; Right Precuneus: $F_{(1,45)} = 27.07$, $p < .001$; Right Mid-cingulate: $F_{(1,45)} = 6.58$, $p < .05$), and a main effect of delay in the left mid-cingulate cortex ($F_{(1,45)} = 4.22$, $p < .05$). In short, for high-confidence responses there is no evidence that the delay affected the magnitude of the retrieval success effect, although there does appear to be indications of an interaction in some regions (by eye), so this analysis may suffer from lack of power.

For completeness, we include the ANOVA for moderate/low confidence hits; here, the conclusions are ambiguous. One PMN region shows a significant interaction (Right Precuneus: $F_{(1,45)} = 5.14$, $p < .05$). Four of the regions show a significant main effect of Hit vs CR (Left Precuneus: $F_{(1,45)} = 14.84$, $p < .001$; Left Mid-cingulate: : $F_{(1,45)} = 9.41$, $p < .01$; Left pIPL: $F_{(1,45)} = 14.00$, $p < .001$; Right Precuneus: $F_{(1,45)} = 19.54$, $p < .001$), and a main effect of delay is seen in bilateral precuneus (Left Precuneus: $F_{(1,45)} = 7.72$, $p < .01$; Right Precuneus: $F_{(1,45)} = 4.24$, $p < .05$).

If an ANOVA is instead performed for only magnitudes of hits with a 2x2 design (Short delay/Long delay vs High/Mod-Low confidence), none of the five PMN regions show a significant interaction (largest $F_{(1,45)} = 0.86$, $p = .36$). A significant main effect of delay is seen in

bilateral precuneus and midcingulate (Left Precuneus: $F_{(1,45)} = 7.26$, $p < .01$; Left Mid-cingulate: : $F_{(1,45)} = 7.81$, $p < .01$; Right Precuneus: $F_{(1,45)} = 5.70$, $p < .05$; Right Mid-cingulate: $F_{(1,45)} = 6.92$, $p < .05$), while a main effect of confidence is seen in two left PMN regions (Left Precuneus: $F_{(1,45)} = 9.13$, $p < .01$; Left pIPL: $F_{(1,45)} = 14.42$, $p < .001$).

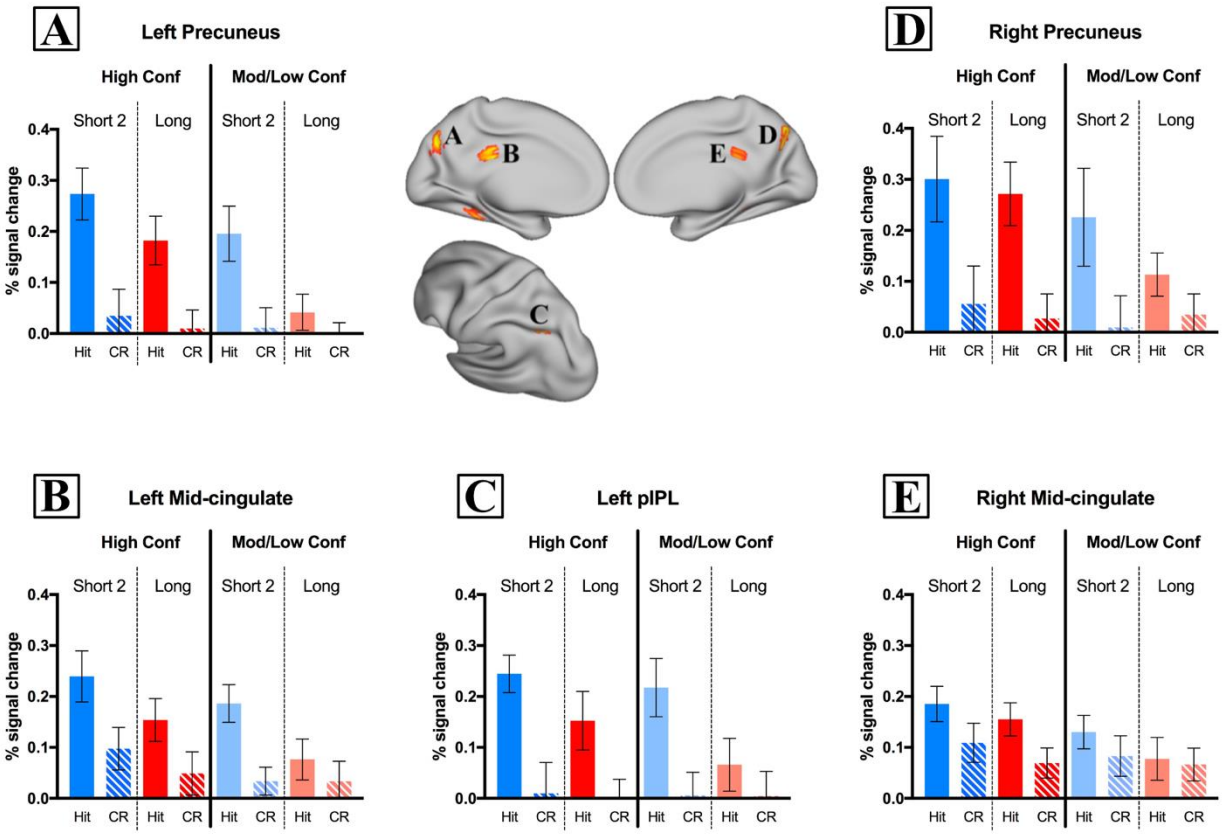

Figure 3.8: Average magnitudes for PMN regions revealed through ANOVA analysis, separated by confidence.

Chapter 4: Discussion

PMN regions have shown a robust retrieval success effect at short retention intervals; however, it is unknown if this contrast is consistent over longer delays between study and test. By administering recognition tests after both short and long retention intervals, we can begin to address this question by comparing patterns of PMN activation during successful remembering of items (hits) compared to correct rejection of lures (CRs).

The initial whole-brain *t*-tests were used to investigate the retrieval success effect at different delays. All three tests (both short delay tests and the long delay test) showed a clear Hit > CR contrast in bilateral PMN regions. The short delay tests replicate multiple previous findings from several meta-analyses, which implicate PMN regions in retrieval success over short retention intervals (Kim, 2013; McDermott, Szpunar, & Christ, 2009; Nelson et al., 2010). Importantly, PMN regions were also clearly visible in the statistical map for the Hit-CR contrast for the long delay. However, this effect appeared to be more robust in the short delay results compared to the long delay results, and so the more targeted masked-ANOVA analysis was used to discover if this conclusion was accurate.

The masked-ANOVA analysis revealed a significant interaction within PMN regions, which indicated a difference in the retrieval success effect between short and long delays. Specifically, the retrieval success effect was present in all PMN regions during a short delay, and was present (but attenuated) in all but one region (right mid-cingulate) for the long delay. That is, in the four regions showing a retrieval success effect during the long delay, there was significantly decreased activation for correctly-remembered items (hits). This decrease appears

to be the cause of the attenuated retrieval success effect over a longer retention interval. In the right mid-cingulate, a similar decrease in activation for hits appears to drive the lack of a retrieval-success effect at the long delay. It is known that the PMN shows less activation when an individual retrieves items with a weaker memory signal (for example, items that have only been studied a single time; see Nelson et al., 2013). It is therefore possible that our delay manipulation is another manifestation of that principle: after a longer delay, a relatively weaker memory signal is manifested by decreased activation even for successfully-retrieval items that (presumably) were encoded just as well as the items tested during the short delay condition.

Additionally, the consideration of confidence is important for the interpretation of these results. Given our primary conclusion above – that the difference in retrieval success is driven by a relative decrease in activation for hits during the long delay – it is important to understand whether this result is modulated by a lack of confidence during the long delay test. There appears to be an inconsistent pattern when responses are split into high confidence and moderate/low confidence. When a 2x2 ANOVA was used to determine the pattern seen in the magnitudes (Hit/CR vs Short delay/Long delay), the retrieval success effect showed no difference over a delay in any PMN region when only high-confidence hits are accounted for; however, the same is true for all but one PMN region for moderate-confidence hits. The main effect of delay varies, although the the main effect of retrieval success was generally seen in all regions across both delays.

When instead comparing a 2x2 ANOVA for hits (Short delay/Long Delay vs High confidence/Mod-low confidence), there was no significant interaction in any region. This lack of interaction implies that the degree of change in activation for hits between the short and long delay does not differ significantly between confidence bins. It is important to note that this

ANOVA is more difficult to interpret, as confidence is not a controlled independent variable, but it lends to the overall picture provided by the analysis of the confidence data.

Taken together, it is challenging to interpret the confidence results. More than likely, this ambiguity is an issue of insufficient power for this level of analysis; with only 16 usable participants, and data broken into finer-grained bins (with fewer observations per cell per subject), it is possible that these unclear results are simply due to the need for a greater number of subjects. However, these results do require us to temper an unrestrained assertion that the difference in the retrieval success effect over delay is due solely to the delay itself. Given the lack of a difference in retrieval success effects between the short and long delays in high-confidence hits, it is possible that the results seen in the initial masked-ANOVA approach are due (in part) to the decrease in confident responses after the delay.

The overall results fit (to some degree) with our initial hypothesis that the memory signal represented in the PMN is temporally constrained. In this case, even a 48 hour delay was enough to significantly decrease the activations in this region elicited by successful recognition of previously-studied items. This attenuation implies that the representation in the PMN is tied to the episodic context in which the item is initially learned, and that some of that context is lost over greater periods of time. It is not possible to tell from our data if this decrease simply reflects a lesser role of the PMN in recognition of memories after a delay, a degredation of the memory signal, or a migration of the memories' representation as is commonly seen in the hippocampal-neocortical consolidation model (Alvarez & Squire, 1994).

In the future, it would be valuable to further extend the delays for PMN experiments of this nature, in order to determine how this effect progresses over time. If this interpretation of the

results is correct, it should be possible to achieve a delay at which recognition successes no longer elicit activation in the PMN, but rather elicit deactivation, which is typically reserved for novel items the first time they encountered (Kim, 2011; Nelson et al., 2013; Otten & Rugg, 2001). In addition, future experiments should be sure to include confidence measures, and seek to frame their results in the context of confidence changes over longer delays.

As we attempt to synthesize the evidence provided by both task-based MRI and functional connectivity studies, it is important that we define the functional roles of these networks. The parietal memory network has received relatively little direct attention in the literature, although a wealth of data exists that hint at the relevant phenomena and boundary conditions to which it is sensitive. It is crucial that we continue to explore the types of tasks that do (and, equally importantly, do not) elicit predictable activity and patterns of activation in this recently-categorized network.

References

Alvarez, P., & Squire, L. (1994). Memory consolidation and the medial temporal lobe: a simple network model. Proceedings of the National Academy of Sciences, 91(15), 7041–7045. https://doi.org/10.1073/pnas.91.15.7041

Chen, H.-Y., Gilmore, A., Nelson, S., & McDermott, K. (2017). Are There Multiple Kinds of Episodic Memory? An fMRI Investigation Comparing Autobiographical and Recognition Memory Tasks. The Journal of Neuroscience, 37(10), 2764–2775. https://doi.org/10.1523/jneurosci.1534-16.2017

Cox, R. (1996). AFNI: Software for Analysis and Visualization of Functional Magnetic Resonance Neuroimages. Computers and Biomedical Research, 29(3), 162–173. https://doi.org/10.1006/cbmr.1996.0014

Doucet, G., Naveau, M., Petit, L., Delcroix, N., Zago, L., Crivello, F., … Joliot, M. (2011). Brain activity at rest: a multiscale hierarchical functional organization. Journal of Neurophysiology, 105(6), 2753–2763. https://doi.org/10.1152/jn.00895.2010

Eklund, A., Nichols, T., & Knutsson, H. (2016). Cluster failure: Why fMRI inferences for spatial extent have inflated false-positive rates. Proceedings of the National Academy of Sciences, 113(28), 7900–7905. https://doi.org/10.1073/pnas.1602413113

Fox, M., Snyder, A., Vincent, J., Corbetta, M., Essen, D., & Raichle, M. (2005). The human brain is intrinsically organized into dynamic, anticorrelated functional networks. Proceedings of the National Academy of Sciences of the United States of America, 102(27), 9673–9678. https://doi.org/10.1073/pnas.0504136102

Gilmore, A., Nelson, S., & McDermott, K. (2015). A parietal memory network revealed by multiple MRI methods. Trends in Cognitive Sciences, 19(9), 534–543. https://doi.org/10.1016/j.tics.2015.07.004

Greicius, M., Krasnow, B., Reiss, A., & Menon, V. (2003). Functional connectivity in the resting brain: A network analysis of the default mode hypothesis. Proceedings of the National Academy of Sciences, 100(1), 253–258. https://doi.org/10.1073/pnas.0135058100

Haist, F., Shimamura, A., & Squire, L. (1992). On the relationship between recall and recognition memory. Journal of Experimental Psychology: Learning, Memory, and Cognition, 18(4), 691. https://doi.org/10.1037/0278-7393.18.4.691

Henson, R. (2005). A mini-review of fMRI studies of human medial temporal lobe activity associated with recognition memory. The Quarterly Journal of Experimental Psychology: Section B, 58(3–4), 340–360. https://doi.org/10.1080/02724990444000113

Henson, R., Rugg, M., Shallice, T., & Dolan, R. (2000). Confidence in recognition memory for words: dissociating right prefrontal roles in episodic retrieval. https://doi.org/10.1162/08989290051137468

Hutchinson, B., Uncapher, M., & Wagner, A. (2015). Increased functional connectivity between dorsal posterior parietal and ventral occipitotemporal cortex during uncertain memory decisions. Neurobiology of Learning and Memory, 117, 71–83. https://doi.org/10.1016/j.nlm.2014.04.015

Kim, H. (2013). Differential neural activity in the recognition of old versus new events: An Activation Likelihood Estimation Meta-Analysis. Human Brain Mapping, 34(4), 814–836. https://doi.org/10.1002/hbm.21474

Konishi, S., Wheeler, M., Donaldson, D., & Buckner, R. (2000). Neural Correlates of Episodic Retrieval Success. NeuroImage, 12(3), 276–286. https://doi.org/10.1006/nimg.2000.0614

Konkle, T., Brady, T., Alvarez, G., & Oliva, A. (2010). Scene Memory Is More Detailed Than You Think. Psychological Science, 21(11), 1551–1556. https://doi.org/10.1177/0956797610385359

Marcus, D., Harwell, J., Olsen, T., Hodge, M., Glasser, M., Prior, F., … Van Essen, D. (2011). Informatics and Data Mining Tools and Strategies for the Human Connectome Project. Frontiers in Neuroinformatics, 5, 4. https://doi.org/10.3389/fninf.2011.00004

McDermott, K., Jones, T., Petersen, S., Lageman, S., & Roediger, I. (2000). Retrieval Success is Accompanied by Enhanced Activation in Anterior Prefrontal Cortex During Recognition Memory: An Event-Related fMRI Study. Journal of Cognitive Neuroscience, 12(6), 965–976. https://doi.org/10.1162/08989290051137503

McDermott, K., Szpunar, K., & Christ, S. (2009). Laboratory-based and autobiographical retrieval tasks differ substantially in their neural substrates. Neuropsychologia, 47(11), 2290–2298. https://doi.org/10.1016/j.neuropsychologia.2008.12.025

Nelson, S., Arnold, K., Gilmore, A., & McDermott, K. (2013). Neural Signatures of Test-Potentiated Learning in Parietal Cortex. The Journal of Neuroscience, 33(29), 11754–11762. https://doi.org/10.1523/jneurosci.0960-13.2013

Nelson, S., Cohen, A., Power, J., Wig, G., Miezin, F., Wheeler, M., … Petersen, S. (2010). A Parcellation Scheme for Human Left Lateral Parietal Cortex. Neuron, 67(1), 156–170. https://doi.org/10.1016/j.neuron.2010.05.025

Peirce, J. (2007). PsychoPy—Psychophysics software in Python. Journal of Neuroscience Methods, 162(1–2), 8–13. https://doi.org/10.1016/j.jneumeth.2006.11.017

Power, J., Cohen, A., Nelson, S., Wig, G., Barnes, K., Church, J., … Petersen, S. (2011). Functional network organization of the human brain. Neuron, 72(4), 665–78. https://doi.org/10.1016/j.neuron.2011.09.006

Power, J. D., Schlaggar, B. L., & Petersen, S. E. (2014). Studying Brain Organization via Spontaneous fMRI Signal. Neuron, 84(4), 681–696. https://doi.org/10.1016/j.neuron.2014.09.007

Raichle, MacLeod, Snyder, Powers, Gusnard, & Shulman. (2001). A default mode of brain function. Proceedings of the National Academy of Sciences, 98(2), 676–682. https://doi.org/10.1073/pnas.98.2.676

Shirer, W., Ryali, S., Rykhlevskaia, E., Menon, V., & Greicius, M. (2012). Decoding Subject-Driven Cognitive States with Whole-Brain Connectivity Patterns. Cerebral Cortex, 22(1), 158–165. https://doi.org/10.1093/cercor/bhr099

Shulman, G., Fiez, J., Corbetta, M., Buckner, R., Miezin, F., Raichle, M., & Petersen, S. (1997). Common blood flow changes across visual tasks: II. Decreases in cerebral cortex. https://doi.org/10.1162/jocn.1997.9.5.648

Smith, S., Beckmann, C., Andersson, J., Auerbach, E., Bijsterbosch, J., Douaud, G., … Consortium, W.-M. (2013). Resting-state fMRI in the Human Connectome Project. NeuroImage, 80, 144–168. https://doi.org/10.1016/j.neuroimage.2013.05.039

Wheeler, M., & Buckner, R. (2004). Functional-anatomic correlates of remembering and knowing. NeuroImage, 21(4), 1337–1349. https://doi.org/10.1016/j.neuroimage.2003.11.001

Yeo, B., Krienen, F., Sepulcre, J., Sabuncu, M., Lashkari, D., Hollinshead, M., … Buckner, R. (2011). The organization of the human cerebral cortex estimated by intrinsic functional connectivity. Journal of Neurophysiology, 106(3), 1125–1165. https://doi.org/10.1152/jn.00338.2011

Yonelinas, A., Otten, L., Shaw, K., & Rugg, M. (2005). Separating the Brain Regions Involved in Recollection and Familiarity in Recognition Memory. The Journal of Neuroscience, 25(11), 3002–3008. https://doi.org/10.1523/jneurosci.5295-04.2005

Appendix

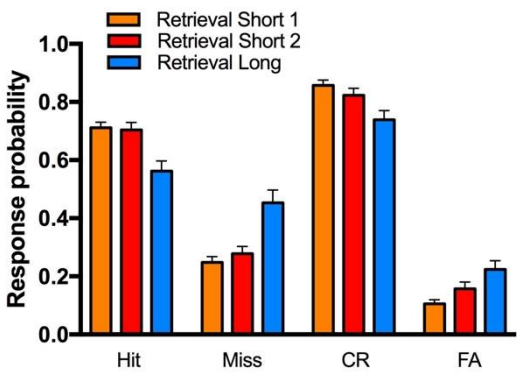

Figure A.1
All behavioral results

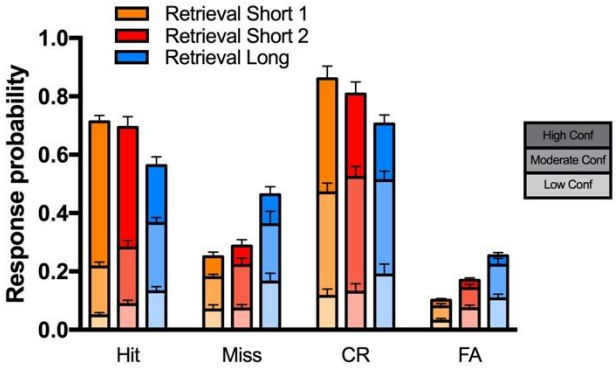

Figure A.2
All behavioral results, separated by confidence

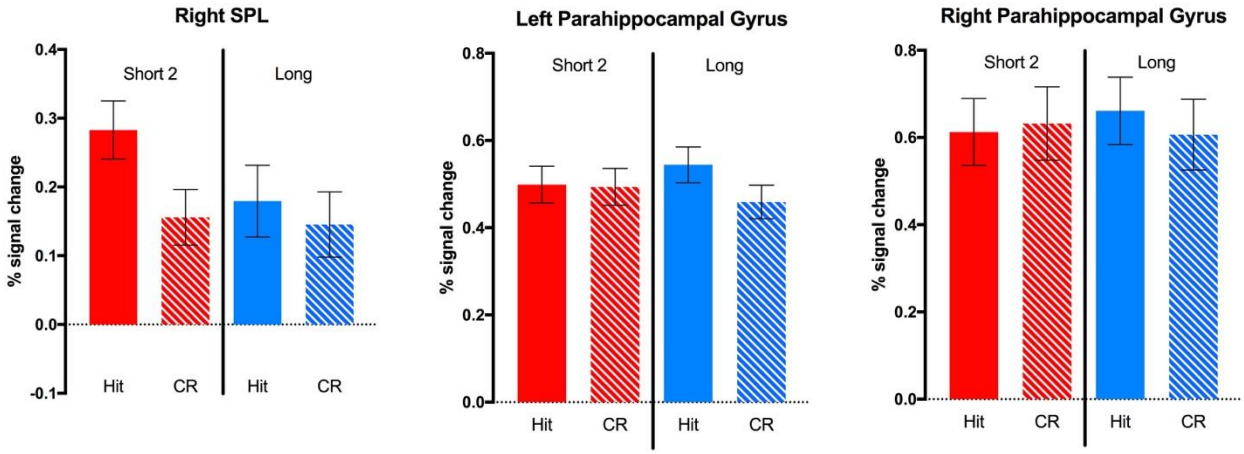

Figure A.3: Average magnitudes for significant non-PMN regions revealed through masked ANOVA analysis (see Figure 3.7 for PMN regions)